Field Measurement of Surface Ship Magnetic Signature Using Multiple AUVs

Benjamin Armstrong, Jesse Pentzer, Douglas Odell*, Thomas Bean, John Canning, Donald Pugsley[+], James Frenzel
Michael Anderson, Dean Edwards
Center for Intelligent Systems Research, University of Idaho, Moscow, ID 83844-1024
*Acoustic Research Detachment, 33964 N. Main Street, Bayview, ID 83803
[+]Carderock Division, Naval Surface Warfare Center, 9500 MacArthur Blvd., West Bethesda, MD 20817-5700

***Abstract*-An effort has been initiated to develop a portable system capable of measuring the magnetic signature of a surface ship. The system will employ a formation of multiple AUVs, each equipped with a magnetometer. The objective is to measure total magnetic field at specified locations relative to the surface ship. In the first step of system development, an Autonomous Underwater Vehicle (AUV) has been equipped with a tri-axial fluxgate magnetometer and used to perform preliminary magnetic field measurements. Measurements of this type will be used to calibrate an individual AUV/magnetometer system. Initial measurements appear to meet necessary measurement requirements on noise floor as the standard deviation of the indicated total magnetic field was observed to be 21nT while the AUV proceeded on a straight, level path. Extended Kalman Filters (EKF) are being developed for on-board AUV navigation and post-processing a best estimate for AUV vehicle position. Navigation experiments were conducted to evaluate AUV navigation and position estimation. In these experiments, an independent high-accuracy topside-track system was used to provide groud-truth for comparison. The average error in the on-board estimated position of the AUV used for navigation was 1.84m. The post processing EKF was designed to use all available sensor data. This EKF had an average position error of 0.74m when compared to the ground-truth. Overall, the AUV was able to navigate to an average distance of 1.95m from its desired waypoint track.**

I. INTRODUCTION

Sea mines represent a dangerous threat to naval vessels. "Since World War II, sea mines have caused more damage to US warships than all other weapons systems combined." [1]. In addition to being effective, sea mines are relatively inexpensive and represent an asymmetric threat.

Sea mines are often triggered by the magnetic field of a passing naval vessel. Consequently, it is of high importance to reduce or mitigate this magnetic field. One way to reduce the magnetic field of a surface vessel is to eliminate sources or to provide active cancellation [2]. A crucial component in the process of signature reduction is magnetic field measurement. Magnetic field measurement is commonly performed at a static electromagnetic range facility equipped with bottom-mounted magnetic sensors [3].

An effort to develop a portable system for measurement of the magnetic field of a naval surface vessel has been initiated. There are several reasons why a portable system would be beneficial. It would reduce the necessity for naval vessels to transit to a range facility for signature measurement. Local measurements could be used to compensate for changes in induced magnetic field caused by variation in the magnetic field of the Earth and geometric re-arrangement of components after a ship leaves a measurement facility.

The approach being employed to develop a portable system for magnetic signature measurement is to equip multiple autonomous underwater vehicles (AUVs) with appropriate sensors and perform a magnetic signature measurement as a formation of AUVs passes beneath a moving surface ship. In the past, it has been reported that AUVs have been equipped with magnetic sensors, mostly for the application of buried mine detection, localization and classification (DLC) [4-7]. This is an application similar to magnetic signature measurement, except that the measured quantity for DLC was magnetic field gradient. For magnetic signature measurement, it is desired to measure total magnetic field over a specified grid of locations relative to the subject surface ship. Recently, an individual AUV was equipped with a magnetic sensor and a signature measurement of a surface vessel was attempted [2]. Magnetic measurements and their corresponding locations were obtained in the experiments, and several areas of future work were identified. Uncertainty in measurement location achieved with the apparatus used was deemed to be too high, and the effect of ship orientation on magnetic signal interpretation was not explored. Also, the time for one vehicle to perform the measurement was thought to be too long.

In the present investigation, efforts are being made to reduce uncertainty in measurement location, to incorporate AUV and ship orientation into magnetic signal interpretation, and to reduce the time for a measurement by using multiple AUVs. Previous developments in cooperative behaviors among multiple AUVs [8,9] will be leveraged to enable coordinated movements between the magnetic sensor equipped AUVs and the surface vessel.

Development of a multi-AUV based magnetic signature measurement system is planned to take place in three segments. In the first segment, a single AUV will be equipped with appropriate sensors and used to measure the magnetic field of a static source. These sensors include a magnetometer and an inertial measurement unit. In the second segment, a single AUV will measure the magnetic field of a moving source, and multiple AUVs will measure the field of a static source. In the third segment, multiple AUVs will be used to measure the field

Report Documentation Page

Form Approved
OMB No. 0704-0188

1. REPORT DATE	2. REPORT TYPE	3. DATES COVERED
OCT 2009		**00-00-2009 to 00-00-2009**

4. TITLE AND SUBTITLE	5a. CONTRACT NUMBER
Field Measurement of Surface Ship Magnetic Signature Using Multiple AUVs	5b. GRANT NUMBER
	5c. PROGRAM ELEMENT NUMBER
6. AUTHOR(S)	5d. PROJECT NUMBER
	5e. TASK NUMBER
	5f. WORK UNIT NUMBER
7. PERFORMING ORGANIZATION NAME(S) AND ADDRESS(ES) **University of Idaho,Center for Intelligent Systems Research,PO Box 441024,Moscow,ID,83844-1024**	8. PERFORMING ORGANIZATION REPORT NUMBER
9. SPONSORING/MONITORING AGENCY NAME(S) AND ADDRESS(ES)	10. SPONSOR/MONITOR'S ACRONYM(S)
	11. SPONSOR/MONITOR'S REPORT NUMBER(S)

12. DISTRIBUTION/AVAILABILITY STATEMENT
Approved for public release; distribution unlimited

13. SUPPLEMENTARY NOTES
Proceedings of Oceans '09 MTS/IEEE Biloxi, Biloxi, Mississippi, October 26-29, 2009. U.S. Government or Federal Rights License

14. ABSTRACT
see report

15. SUBJECT TERMS

16. SECURITY CLASSIFICATION OF:			17. LIMITATION OF ABSTRACT	18. NUMBER OF PAGES	19a. NAME OF RESPONSIBLE PERSON
a. REPORT	b. ABSTRACT	c. THIS PAGE			
unclassified	**unclassified**	**unclassified**	**Same as Report (SAR)**	**9**	

of a moving source. The following sections describe the modifications made to the AUVs for making magnetic measurements and the navigation algorithms used are described. Finally, a description of the testing facility is provided and results obtained in the completion of the first segment of development are shown.

II. MULTIPLE-AUV SIGNATURE MEASUREMENT APPROACH

It is planned to perform a magnetic signature measurement in successive passes of relative motion between a formation of AUVs and a surface ship. The surface ship and formation will intercept on parallel paths through a given measurement area. The AUV formation geometry will be designed to ensure measurements at given grid points relative to the surface ship. The grid points will be placed on parallel paths with a separation of 3m, and the AUVs will be required to adhere to these paths to an accuracy of ±1m. The goal is to locate the AUV relative to the ship within a tolerance of ±1m. If the formation consists of seven AUVs, each separated by 3m, a measurement area with a width of 17.5m (57.4ft) may be covered in a single pass.

While proceeding on parallel paths, measurements of total magnetic field will be performed. The required range of total field measurement is ±100,000nT, and the threshold noise floor is 100nT (goal 25nT). Multiple passes at chosen cardinal directions will be completed.

During an individual pass between the formation and surface ship, the AUV formation will be at beam's depth, within ±1m. While underwater, the AUVs will acquire ranges from acoustic transponders attached to the surface ship to supplement other navigation sensors on the AUV. Presently, underwater experiments are being conducted using acoustic round-trip time-of-flight ranging, but in the second segment of the system development utilization of one-way time-of-flight acoustic range measurement is planned [10].

After performing a measurement, magnetic signal interpretation will be performed by post-processing time-synchronized AUV and ship sensor data.

III. AUVS AND SENSORS

The following describes the AUVs adapted to perform magnetic measurements. The on-board navigation system and post processing navigation systems are also described. The on-board navigation system utilized limited information and is slowly being updated to a more complex system as field testing allows. The post processing navigation system utilized all available information and allows for simulation of system changes before implementation into the AUV.

A. AUV

Fig. 1 shows one of the AUVs adapted to measure magnetic signatures. The AUVs are modified versions of the vehicles built by Dan Stillwell of Virginia Tech. The AUVs are approximately 1m (39in) long and 10cm (4in) in diameter and were controlled by a distributed processing network consisting of five microcontrollers. The heading of the AUV was measured with a magnetic compass utilizing magnetoresistance technology [11] and capable of an accuracy of ±0.5° when properly compensated. Two micro-electro-mechanical (MEMS) accelerometers [12] provided pitch and roll measurements. A capacitive type [13] pressure sensor provided depth measurements to an accuracy of ±0.0879m, and a GPS unit was used to provide position information while on the surface. A six axis inertial measurement unit (IMU) was added to provide improved position estimates between navigation fixes. The IMU uses solid state MEMS accelerometers and gyros [12] measured angular rates and accelerations about three orthogonal axes with accuracies of 0.0006°/sec and 50μg, respectively. Time-of-flight measurements to transponders at known locations were taken by an acoustic Micro-modem [14,15] designed and built by the Woods Hole Oceanographic Institute.

The magnetometer mounted on the AUVs, shown in Fig. 1, was a three-axis fluxgate type [16] magnetometer with a range of ±100,000 nT and a sensitivity of 100μV/nT. The accuracy of the magnetometer was ±0.5% of full scale while the orthogonality between sensitive axes was <±1°.

The AUVs were equipped with a data acquisition unit (DAQ) for sampling and storing the data from the magnetometer. The DAQ was comprised of multiple D.Module boards from D.SignT: (1) a C6713 processor board, (2) a AD7722 Analog to Digital Conversion (ADC) board, and (3) a 91C111 network and storage board. The processor board included a TI TMS3206713 DSP running at 300 MHz with 2 MB of flash memory and 32 MB of SDRAM. The ADC board supported six channels at 16-bit resolution and up to 200 ksps. The network and storage board enabled Ethernet-control of the recording operation and 2 GB of storage on a flash memory card. For our purposes, each component of the magnetometer was sampled at a rate of 12.5K samples per second and 16-bit resolution, providing a magnetic resolution of 3 nT/LSB. The external storage card could store 400 minutes (6.7 hours) of data at this rate and resolution. In order to maintain uninterrupted data recording, a software buffering scheme was utilized.

B. AUV Control

The AUVs used classical proportional controllers to maneuver to the proper depth and to follow a set of waypoints.

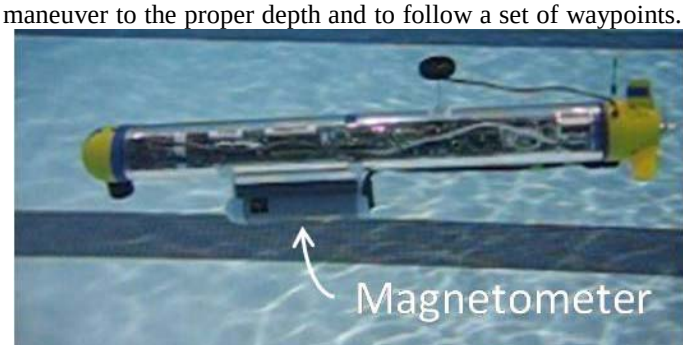

Figure 1. Magnetometer equipped AUV during pool testing at the University of Idaho

The control systems on the AUV were treated separately as two uncoupled controllers: a depth controller and a heading controller.

The depth controller maintained the commanded depth using a proportional controller on pitch error and proportional and integrator controls on depth error. The control problem is presented in Fig. 2. The control law may be expressed as

$$\delta_{\mathrm{E}} = \mathrm{P_z}(\mathrm{z_{ref}} - \mathrm{z}) + \mathrm{I_z}\int_{\mathrm{t}}(\mathrm{z_{ref}} - \mathrm{z})\ \mathrm{dt} + \mathrm{P_\theta}(\theta_{\mathrm{ref}} - \theta), \quad (1)$$

where z was the measured depth, and θ was the measured pitch of the vehicle. The desired depth and pitch were $\mathrm{z_{ref}}$ and θ_{ref}, respectively. $\mathrm{P_z}$, $\mathrm{I_z}$, and P_θ were the control constants for the proportional and integral controls on depth and the proportional control on pitch. These terms combined as shown in the equation to arrive at the elevator control surface position, δ_{E}.

The heading controller for the vehicles was based on a controller system that is available in the MOOS platform [17] developed at the Massachusetts Institute of Technology. The control system was simply a proportional heading controller to match the heading of the vehicle to the recommended heading. However the recommended heading was found by geometry as shown in Fig. 3. The control law can be expressed simply as

$$\delta_{\mathrm{R}} = \mathrm{P}_\psi(\psi_{\mathrm{ref}} - \psi) \quad (2)$$

where ψ represented the heading of the vehicle. The recommended heading was ψ_{ref}, and the control constant was P_ψ. These values combined to form the recommended rudder angle, δ_{R}. The recommended heading, ψ_{ref}, was the direction of a vector drawn from current vehicle location to a point on the waypoint path that was a specified distance beyond the closest point on the path. This distance is represented in Fig. 3 as $d_{lookahead}$.

C. AUV Navigation and Extended Kalman Filter

The AUV navigated with the use of a discrete time Extended Kalman Filter (EKF) [18]. The EKF propagates with the system model

$$X_k = f_{k-1}(X_{k-1}, u_{k-1}, w_{k-1}), \quad (3)$$

where X is the system state, u is the control input and w is the process noise covariance. The process noise covariance is defined as $w_k \sim (0, Q^2)$where Q is the standard deviation. The EKF updates with an observation model

$$y_k = h_k(X_k, v_k), \quad (4)$$

where v is the update measurement covariance. The update covariance is defined as $v_k \sim (0, R^2)$where R is the standard deviation of the measurement. The state and error covariance are propagated with

$$P_k^- = F_{k-1}P_{k-1}^+F_{k-1}^T + L_{k-1}Q_{k-1}L_{k-1}^T\,, \quad (5)$$

$$x_k^- = f_{k-1}(x_{k-1}^+, u_{k-1}, 0), \quad (6)$$

where P is the system covariance. F and L are defined as

$$F_{k-1} = \frac{\partial f_{k-1}}{\partial x}\Big|_{x_{k-1}^+}, L_{k-1} = \frac{\partial f_{k-1}}{\partial w}\Big|_{x_{k-1}^+}. \quad (7,8)$$

The state updates with measurements through

$$K_k = P_k^-H_k^T(H_kP_k^-H_k^T + M_kR_kM_k^T)^{-1}\,, \quad (9)$$

$$x_k^+ = x_k^- + K_k[y_k - h_k(x_k^-, 0)], \quad (10)$$

$$P_k^+ = (I - K_kH_k)P_k^-. \quad (11)$$

H and M are defined as

$$H_k = \frac{\partial h_k}{\partial x}\Big|_{x_k^-}, M_k = \frac{\partial h_k}{\partial v}\Big|_{x_k^-}. \quad (12,13)$$

The EKF operating on the AUV used a simple kinematic continuous time model

$$\dot{N} = s\cos\psi,\ \dot{E} = s\sin\psi, \quad (14,15)$$

$$\dot{s} = 0, \dot{\psi} = 0\,, \quad (16,17)$$

where $\dot{N}$ and $\dot{E}$ were the velocities in the North and East directions, respectively, s was speed, and ψ was heading. The state vector for the kinematic model was

$$X = \{N \quad E \quad s \quad \psi\}^T. \quad (18)$$

Using the Euler approximation of the time derivative, the discrete system model was

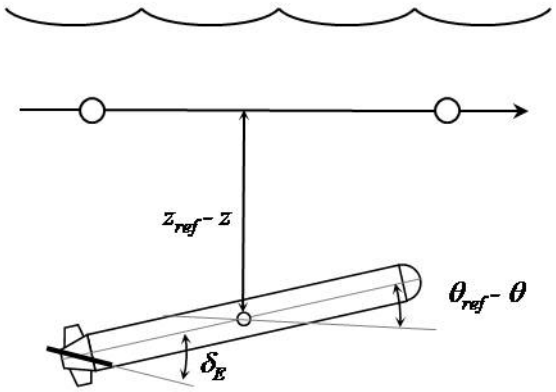

Figure 2. Depth Control Problem

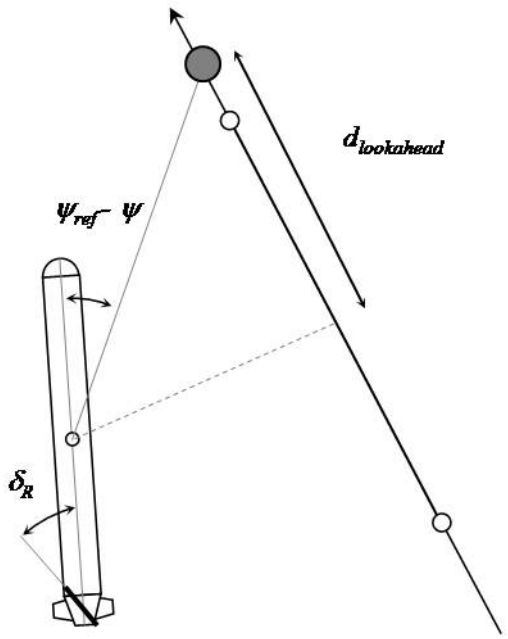

Figure 3. Heading Control Problem

$$X_k = f(X,u,w)_{k-1} = \begin{Bmatrix} \Delta t\ s\ cos\psi + N + w_E \\ \Delta t\ s\ sin\psi + E + w_N \\ s + w_s \\ \psi + w_\psi \end{Bmatrix}_{k-1}, \quad (19)$$

where Δt was the discrete time step.

The available measurements were

$$y = \{r_1 \quad r_2 \quad r_3 \quad r_4 \quad s \quad \psi\}^T \quad (20)$$

where $r_{1\text{-}4}$ were acoustic ranges to fixed transponders at known locations, the speed s was converted from propeller RPM using a linear fit, and ψ was the compass heading. The measurements were related to the states using

$$y = \begin{Bmatrix} \sqrt{(N-B_{N1})^2 + (E-B_{E1})^2 + (Z-B_{Z1})^2} + v_{r1} \\ \sqrt{(N-B_{N2})^2 + (E-B_{E2})^2 + (Z-B_{Z2})^2} + v_{r2} \\ \sqrt{(N-B_{N3})^2 + (E-B_{E3})^2 + (Z-B_{Z3})^2} + v_{r3} \\ \sqrt{(N-B_{N4})^2 + (E-B_{E4})^2 + (Z-B_{Z4})^2} + v_{r4} \\ s + v_s \\ \psi + v_\psi \end{Bmatrix} \quad (21)$$

where B_N, B_E, and B_Z were the North position, East position, and depth of the transponders, respectively, and Z was the depth measurement from the pressure sensor.

The EKF propagated and updated at a rate of 4 Hz which was the rate of the compass and propeller RPM measurements. The range measurements occurred at 30 second intervals and, depending on the number of replies received, anywhere from zero to four were added to the observation model depending on availability.

D. Post Processing Extended Kalman Filter

An EKF that used all available information recorded by the AUV was used to post process the sensor and range data to improve the position estimate. The state vector in the post process EKF was

$$X = \{N \ \ E \ \ Z \ \ \dot{N} \ \ \dot{E} \ \ \dot{Z} \ \ \phi \ \ \theta \ \ \psi \ \ \delta_x \ \ \delta_y \ \ \delta_z\}^T \quad (22)$$

where N, E, Z and $\dot{N}$, $\dot{E}$, $\dot{Z}$ were the vehicle positions and velocities in the North, East, and downward directions, respectively; ϕ, θ, and ψ were the Euler angles of roll, pitch, and heading, respectively; and δ_x, δ_y, and δ_z were IMU accelerometer offsets in the body x, y, and z directions, respectively. The a_x, a_y, and a_z accelerations and ω_x, ω_y, and ω_z angular rate outputs of the IMU were aligned with the AUV x-y-z axes as shown in Fig. 4.

The continuous time model was developed by transforming the IMU accelerations into the inertial frame and the angular rates into Euler angle rates. The three measured angular rates ω_x, ω_y, and ω_z were transformed into the Euler angle rates $\dot{\phi}$, $\dot{\theta}$, and $\dot{\psi}$ using [19]

$$\begin{Bmatrix} \dot{\phi} \\ \dot{\theta} \\ \dot{\psi} \end{Bmatrix} = R_\omega \begin{Bmatrix} \omega_x + w_{\omega_x} \\ \omega_y + w_{\omega_y} \\ \omega_z + w_{\omega_z} \end{Bmatrix} \quad (23)$$

where

$$R_\omega = \begin{Bmatrix} 1 & sin\phi tan\theta & sin\phi tan\theta \\ 0 & cos\phi & -sin\phi \\ 0 & sin\phi sec\theta & cos\phi sec\theta \end{Bmatrix} \quad (24)$$

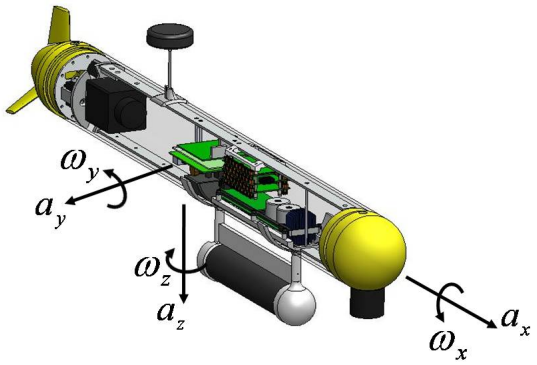

Figure 4. AUV and IMU coordinate system

is the non-orthogonal transformation used for this purpose and w_{ω_x}, w_{ω_y}, and w_{ω_z} are process noise covariance variables required by the EKF.

The acceleration measurements were rotated from the vehicle x-y-z axes to the inertial N-E-Z axes using [19]

$$\begin{Bmatrix} \dot{N} \\ \ddot{E} \\ \ddot{Z} \end{Bmatrix} = R_a \begin{Bmatrix} a_x + \delta_x + w_{a_x} \\ a_y + \delta_y + w_{a_y} \\ a_z + \delta_z + w_{a_z} \end{Bmatrix}, \quad (25)$$

where w_{a_x}, w_{a_y}, and w_{a_z} are once again process noise covariance parameters and

$$R_a = \begin{Bmatrix} c\psi c\theta & -s\psi c\phi + c\psi s\theta s\phi & s\psi c\phi + c\psi s\theta c\phi \\ s\psi c\theta & c\psi c\phi + s\psi s\theta s\phi & -c\psi s\phi + s\psi s\theta c\phi \\ -s\theta & c\theta s\phi & c\theta c\phi \end{Bmatrix} \quad (26)$$

is the rotation matrix where c and s represent sine and cosine, respectively. The continuous time system model was formed by combining (23) and (25) with

$$\begin{Bmatrix} \dot{\delta}_x \\ \dot{\delta}_y \\ \dot{\delta}_z \end{Bmatrix} = \begin{Bmatrix} 0 \\ 0 \\ 0 \end{Bmatrix}, \quad (27)$$

which allowed the accelerometer offsets to be adjusted by the filter.

Using the Euler approximation of the time derivative, the discrete time form of the system model can be derived from (23), (25), and (27) as

$$X_k = f(X,u,w)_{k-1} = \begin{Bmatrix} N + \Delta t\dot{N} \\ E + \Delta t\dot{E} \\ Z + \Delta t\dot{Z} \\ \begin{bmatrix} \dot{N} \\ \dot{E} \\ \dot{Z} \end{bmatrix} + \Delta t R_a \begin{bmatrix} a_x + \delta_x + w_{a_x} \\ a_y + \delta_y + w_{a_y} \\ a_z + \delta_z + w_{a_z} \end{bmatrix} \\ \begin{bmatrix} \phi \\ \theta \\ \psi \end{bmatrix} + \Delta t R_\omega \begin{bmatrix} \omega_x + w_{\omega_x} \\ \omega_y + w_{\omega_y} \\ \omega_z + w_{\omega_z} \end{bmatrix} \\ \delta_x + w_{\delta_x} \\ \delta_y + w_{\delta_y} \\ \delta_z + w_{\delta_z} \end{Bmatrix}_{k-1} \quad (28)$$

The variables a_x, a_y, a_z, ω_x, ω_y, ω_z, δ_x, δ_y, and δ_z were classified as control inputs to the system.

The measurements available to the system were

$$y = \{r_1 \quad r_2 \quad r_3 \quad r_4 \quad z \quad s \quad \phi \quad \theta \quad \psi \quad \psi\}^T \quad (29)$$

where $r_{1\text{-}4}$ were again acoustic ranges to fixed transponders at known locations, z was the depth measured by the pressure transducer, the speed s was converted from propeller RPM using a first order relationship, ϕ was the roll sensor measurement, θ was the pitch sensor measurement, and ψ was the compass heading. The measurements were related to the states using

$$y = \begin{Bmatrix} \sqrt{(N - B_{N1})^2 + (E - B_{E1})^2 + (Z - B_{Z1})^2} + v_{r1} \\ \sqrt{(N - B_{N2})^2 + (E - B_{E2})^2 + (Z - B_{Z2})^2} + v_{r2} \\ \sqrt{(N - B_{N3})^2 + (E - B_{E3})^2 + (Z - B_{Z3})^2} + v_{r3} \\ \sqrt{(N - B_{N4})^2 + (E - B_{E4})^2 + (Z - B_{Z4})^2} + v_{r4} \\ Z + v_z \\ \sqrt{\dot{N}^2 + \dot{E}^2 + \dot{Z}^2} + v_s \\ \phi + v_\phi \\ \theta + v_\theta \\ \psi + v_{\psi 1} \\ \operatorname{atan}\left(\frac{\dot{E}}{\dot{N}}\right) + v_{\psi 2} \end{Bmatrix} \quad (30)$$

where B_N, B_E, and B_Z were again transponder locations and the subscripted v variables represented the measurement noise covariances required by the EKF. The purpose of the second heading measurement was to force the majority of the velocity of the AUV to be tangent to the path of the AUV.

The four range measurements were available every two seconds while the rest of the measurements were available at 4Hz. Therefore, the EKF adjusted the size of the necessary arrays to match the number of measurements available at each time step.

IV. TEST RANGE

Bayview, Idaho is the home of the Acoustic Research Detachment (ARD) of the Naval Surface Warfare Center, Carderock Division. Lake Pend Oreille provides a unique research environment with sheltered waters, low ambient noise, and low absorption losses. Facilities at Bayview include two long-baseline tracking range areas, one in shallow water (15m depth) and one in deep water (350m depth). A third range area is under development, at a depth of 200m. The shallow-water range is used for the majority of AUV testing. Each range is instrumented with bottom-mounted tracking nodes which are cabled to shore-based tracking systems. Each node can function as receiver, transmitter, and transponder. Each range can track multiple vehicles, each vehicle being equipped with an acoustic pinger. Tracking can be synchronous (known ping time) or asynchronous (unknown ping time).

Acoustic tracking requires measurement of acoustic propagation delay and knowledge of sound velocity. For a typical tracking application, acoustic ping waveforms are periodically transmitted from each vehicle (AUV). From each ping, distance is measured to multiple known locations (tracking nodes). Vehicle location is then computed using least-squares or other standard techniques.

Tracking accuracy can be effected by many factors. Some of these include sound velocity errors, multipath contamination, Doppler shift, ping waveform characteristics, and acoustic receiver design. Shallow-water ranges are characterized by high multipath contamination caused by surface and bottom reflections. ARD ranges incorporate unique features to reduce tracking error. Each bottom-mounted tracking node includes an acoustic backing plate mounted below the transducers to suppress reflections from the lake bottom and node structure. A self-survey technique is used to accurately measure the location and depth of each node. To combat the shallow-water multipath problem, an acoustic receiver algorithm was developed which combines both correlation and leading-edge techniques.

Depending on user requirements, tracking accuracy can be measured in different ways. It is often most important to know the relative location and/or velocity of two submerged objects. ARD acoustic ranges excel at this – with accuracies of 0.1 m demonstrated at the deep-water range. Accuracies of 0.2 m are possible for AUV tracking in the shallow-water range. Surface waves and vehicle motion cause the underwater acoustic environment to continually change. These changes affect accuracy. Occasional errant track points are statistically unavoidable.

The majority of field testing was conducted in the shallow-water range located at the south end of the lake. A frequency band of 22-28 kHz is used, with acoustic source levels ranging from 180-185 dB (re: 1 μPa@1 m). The absorption coefficient in fresh water at this frequency band is approximately 0.15 (dB/km). Sea state conditions of 0-1 were typical during tests with wave height less than 0.1 m. The bottom composition is sandy silt. Depending on weather, the sound velocity profile can change rapidly. Underwater ambient noise levels are generally dominated by recreational boat traffic. However, a large no-wake zone keeps high-speed boat traffic approximately 1500 m from the shallow-water range area.

The shallow-water range area is located inside the secured marina containing the docks for the base. The total area available for maneuvering within these waters measures about 130 meters in length and about 100 meters in width. The primary course is three sides of a rectangle that would represent two scans of a lawnmower search with a total length of 190 meters. To best use the available area inside the ARD, the rectangle is rotated such that the first 80 meter leg is in the southeast direction (135º). The vehicle turns 90 degrees to the right and travels the 30 meters in the southwest direction (225º) to arrive at the beginning of the second 80 meter leg which is oriented in the northwest direction (315º). .

V. RESULTS

A. Magnetometer Measurements in Constant Field

Initial measurements with one AUV have been taken in a static Earth field. The measurements were taken in open water to remove magnetic field anomalies caused by buildings, boats, pilings, etc. The purpose of the measurements was to obtain magnetometer readings that could be used to perform calibration calculations on the AUV system. The calibration

procedure produces a gain matrix and a set of offsets by matching experimental data with the static field assumption. The gain matrix and offset parameters are allowed to vary until an optimal fit is attained between the experimental data and a static field. The calibration requires that the experimental data include measurements taken while the AUV is undergoing changes in heading, pitch, and roll that would be observed during normal operation. A circular test path was chosen for this reason as it allowed the AUV to complete a 360° heading change while pitching and rolling as it would during an operational turn.

Fig. 5 shows the path of the AUV while operating one meter under the surface. After the dive was completed, the AUV travelled at a fairly constant heading to get away from any magnetic anomalies on the launching boat. Fig. 6a shows the magnetic data recorded on the three axes and the calculated total field versus time while Fig. 6b shows the heading, pitch, and roll of the AUV versus the same time scale. A fifth-order Chebyshev type two non-causal lowpass filter with a cutoff attenuation of 1dB and a cutoff frequency of 5Hz was used to filter the magnetic data [20]. For reference, Fig. 7 shows the nominal relative orientation of the sensitive axes of the magnetometer with the AUV. The *Z* axis was aligned with the body of the vehicle while the *Y* and *X* axes were nominally vertical and horizontal. Looking at Fig. 6b, the AUV travelled at a heading of approximately 130° for 30 seconds. The labeled

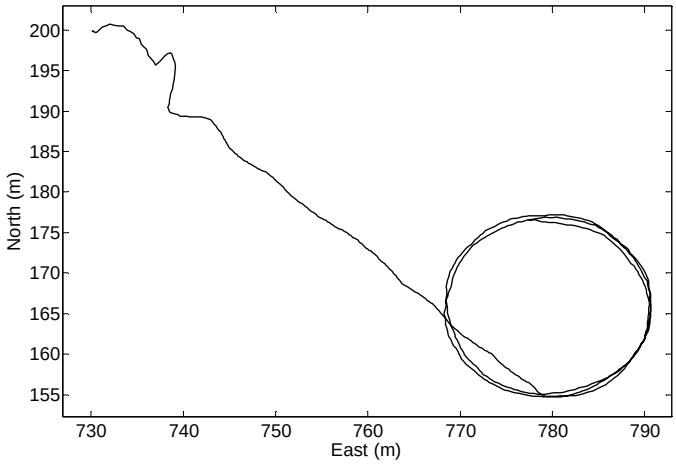

Figure 5. AUV magnetic measurement path while traveling underwater

gaps in the magnetic and attitude data are due to a recording constraint that had been solved at the time of writing this paper. After travelling at constant heading, the AUV set a constant rudder angle and began making counter-clockwise circles. The changing orientation of the AUV relative to magnetic field of the Earth is reflected in the changing values of the *X* and *Z* field magnitudes shown in Fig. 6a. The oscillations are approximately 90° out of phase due to the orthogonal alignment of the two sensitive axes.

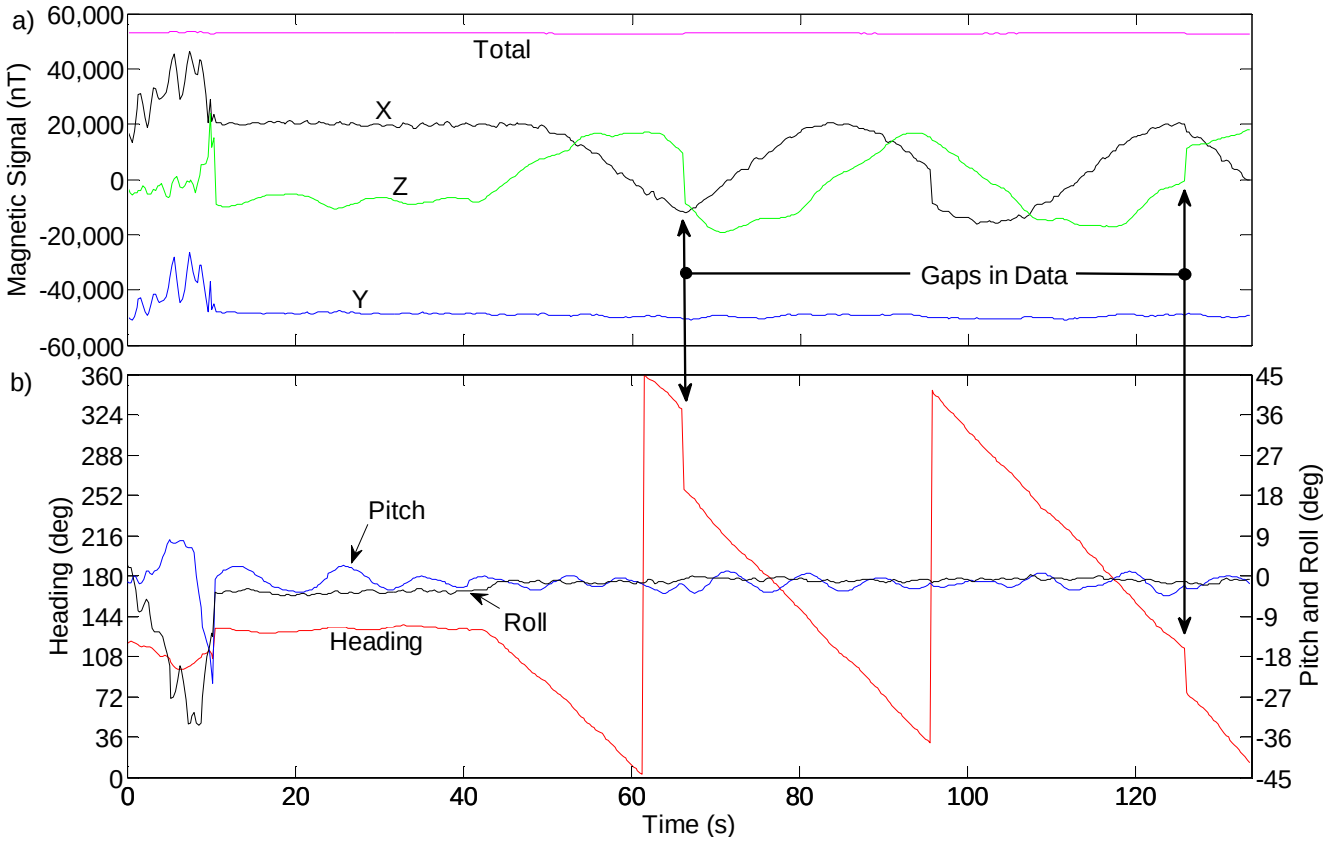

Figure 6. Experimental magnetometer data with corresponding vehicle attitude a)*X,Y,Z* components and total magnetic field magnitudes b)Heading, pitch, and roll of AUV

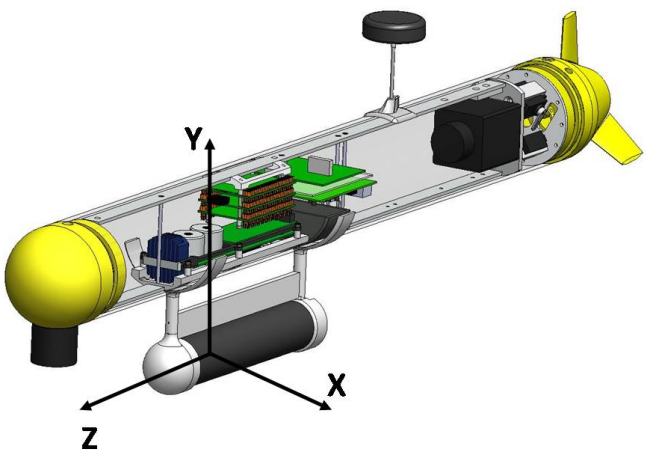

Figure 7. Orientation of magnetometer axis in relation to AUV

Fig. 8 shows the total field magnitude and corresponding heading data from Fig. 6, only now the limits of the vertical axes have been narrowed to show signal detail. During the constant heading portion of the test run, 10s-40s, the measured total field magnitude averaged 52,995nT with a standard deviation of 21nT. Fig. 8 shows that there were oscillations in the total field as the AUV changed heading. The largest deviations in the total field were -475nT and -425nT at 61.50 seconds and 95.75 seconds, respectively. Both of the largest deviations occurred when the heading of the AUV was near 0°, or north.

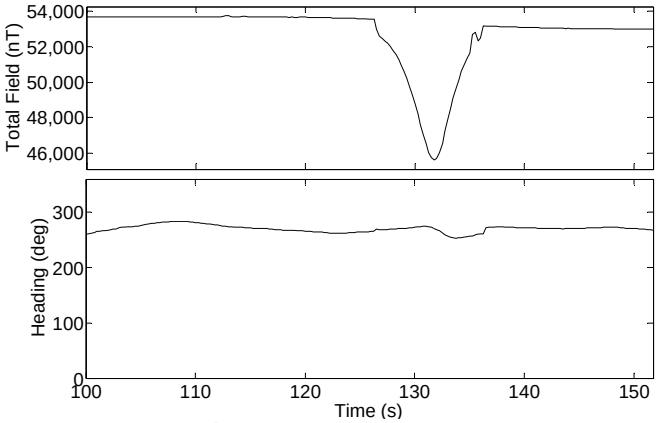

Figure 9. Total field measurement of a steel piling at ~1.5m and AUV heading

B. Measurement of Changing Field

A simple test to measure a changing field was performed by running the AUV near a large steel piling in the test area. The resulting total field and heading data is shown in Fig. 9. The closest point of approach to the piling was approximately 1.5m. As shown in Fig. 9, the largest deflection in the total field occurred in the time interval 126 – 136 seconds and had a magnitude of ~8000nT. It is important to note that the compass also deviated by approximately ±10° during the test, as shown in Fig. 9.

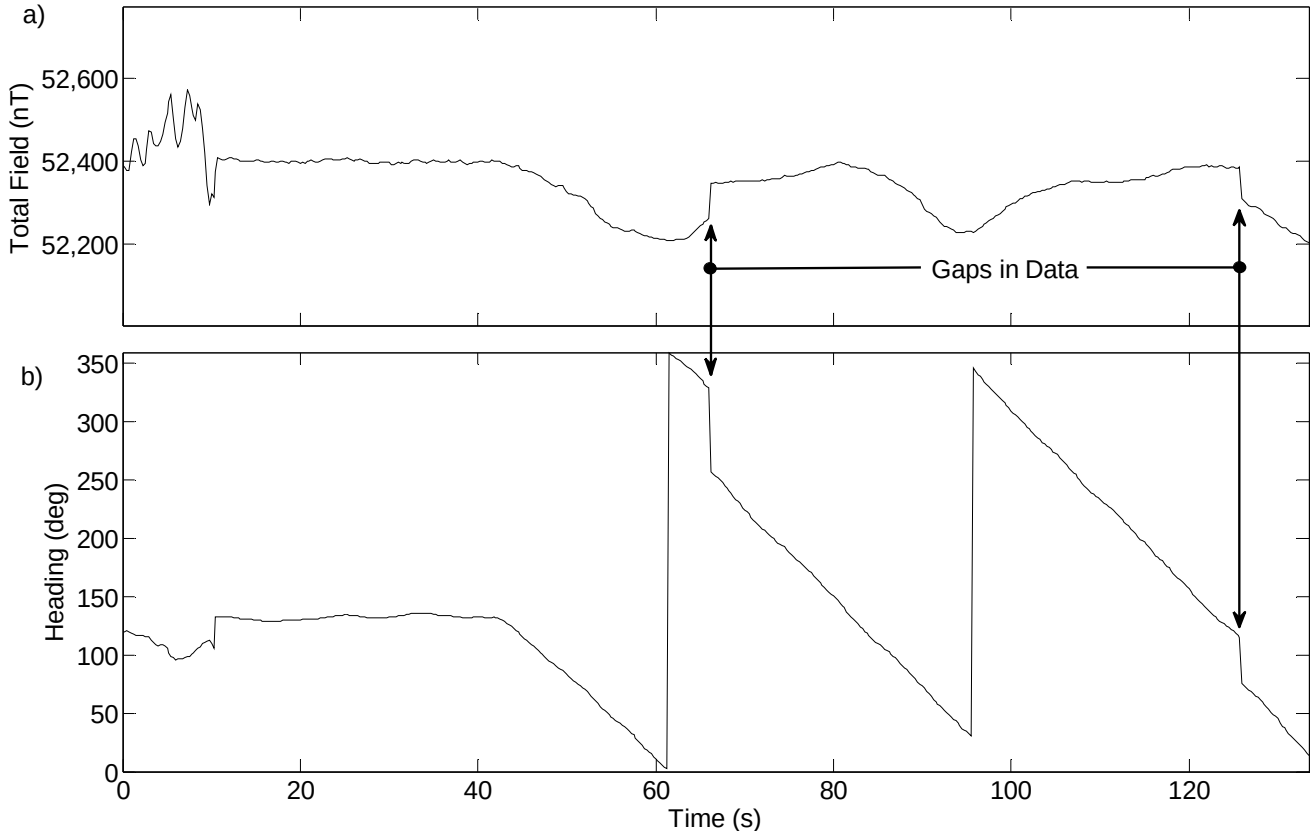

Figure 8. Experimental magnetometer data with corresponding vehicle heading
a)Total magnetic field magnitudes b)Heading of AUV

C. Navigation Performance

Fig. 10 shows a comparison of EKF position estimates used by the on-board AUV controller, the post-processed EKF position estimate, the topside ground truth, and the intended waypoint path. The average error between the AUV controller and the topside track was 1.84m, and the average error between the post process EKF and the topside track was 0.74m. For this data the AUV controller received ranges at 30 second intervals while the post process EKF received ranges at 2 second intervals.

It is important that the navigation controllers navigate the AUV closely to the desired waypoint path so that proper spacing can be maintained while taking magnetic signature measurements. In Fig. 10, the average perpendicular distance between the waypoint track and the AUV controller path was 1.51m. The average perpendicular distance between the topside solutions and the waypoint path was 1.95m, which shows that the AUV controller track was closer to the path than the actual vehicle path. The average perpendicular distance for the post process EKF was 1.88m, which agrees with the fact that the post process EKF track matched the topside solution points much closer than the AUV controller.

VI. Summary, Conclusions and Future Work

An AUV has been equipped to collect magnetic measurements while accurately navigating relative to a waypoint course. Test data was collected which will allow for compensation of the induced magnetic field of the AUV. Initial measurements taken with the on-board magnetometer show that when traveling in a straight line, the measured signal has a standard deviation of 21nT, which is within project specifications. However, there exists an abnormality when traveling at a heading near 0°. A pass-by test of a steel piling produced the desired deviation with an appropriate magnitude.

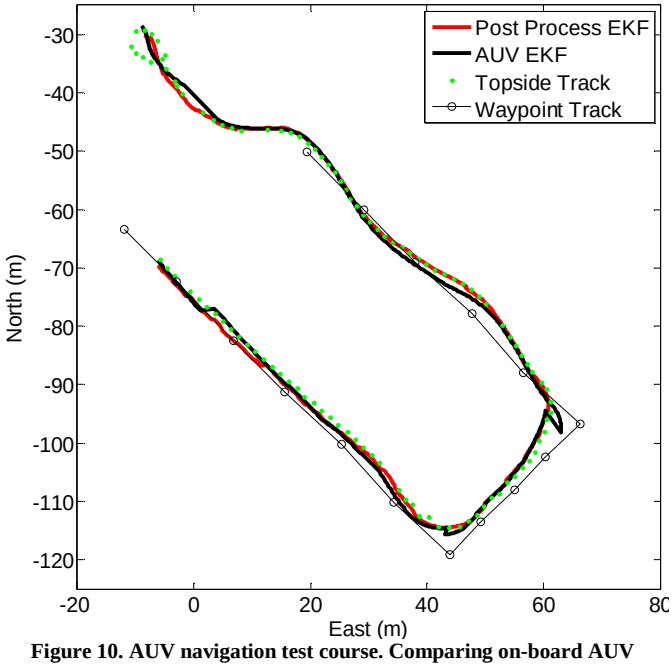

Figure 10. AUV navigation test course. Comparing on-board AUV controller, post-processed EKF, topside ground truth, and desired waypoint track

The AUV on-board navigation was able to achieve an average position accuracy of 1.84m when compared to the topside track. A post process EKF was able to improve upon this such that the average error was within 0.74m. The navigation controller was able to maneuver the vehicle to an average perpendicular distance between the topside and waypoint path of 1.95m.

Future work includes developing the DAQ, calibrating the on-board magnetometer, and expanding to AUV fleet operations. The on-board EKF will operate with received ranges at 2 second intervals to increase accuracy. The IMU will be calibrated to improve the post process EKF. The AUVs induced magnetic field will be calculated and removed from future measurements.

Acknowledgment

The authors gratefully acknowledge the support of the Office of Naval Research, through "Electromagnetic Signature Assessment System Using Multiple Autonomous Underwater Vehicles (AUVs)", ONR N00014-08-1-0779.

References

[1] US Department of Defense, "Unmanned System Roadmap 2007-2032", December 10, 2007.

[2] J.J. Holmes, "Exploitation of a Ship's Magnetic Field Signatures", Morgan & Claypool Publishers, 2006.

[3] J. B. Nelson, T.C. Richards, "Magnetic Source Parameters of MR OFFSHORE Measured During Trial MONGOOS 07", Defense R&D Canada-Atlantic, 2007.

[4] G.I. Allen, B. Sulzberger, J.T. Bono, J.S. Pray, T.R. Clem, "Initial Evaluation of the New Real-time Tracking Gradiometer Designed for Small Unmanned Underwater Vehicles", Oceans 2005 Proceedings of IEEE/MTS, Vol. 3, pp. 1956-1962, 2005.

[5] G.I. Allen, R. Mattews, M. Wynn, "Mitigation of Platform Generated Magnetic Noise Impressed on a Magnetic Sensor Mounted in an Autonomous Underwater Vehicle", Oceans 2001 Proceedings of IEEE/MTS, Vol. 1, pp. 63-71, 2001.

[6] T.R. Clem, J.L. Lopes, "Progress in the Development of Buried Minehunting Systems", Oceans 2003 Proceedings, Vol. 1, pp. 500-511, 2001.

[7] R. Wiegert, "Magnetic Anomaly Guidance System for Mine Countermeasures Using Autonomous Underwater Vehicles", Oceans 2003 Proceedings, Vol. 4, pp. 2002-2010, 2003.

[8] T. Bean, G. Beidler, J. Canning, D. Odell, R. Wall, M. O' Rourke, M. Anderson, D. Edwards, "Language and Logic to Enable Collaborative Behavior among Multiple Autonomous Underwater Vehicles", *The International Journal of Intelligent Control and Systems*, Vol. 13, No. 1, pp. 67-80, 2008.

[9] T. Bean, J. Canning, G. Beidler, M. O' Rourke, D. Edwards,"Designing and Implementing Collaborative Behaviors for Autonomous Underwater Vehicles", Proceedings of UUST07, Lee, NH, August 19-22, 2007.

[10] R.M. Eustice, L.L. Whitcomb, H. Singh, and M. Grund, "Experimental Results in Synchronous-clock One-Way-Travel-time Acoustic Navigation for Autonomous Underwater Vehicles", *IEEE Intl. Conf. Robotics & Automation*, April, 2007.

[11] J. Lenz, "A review of magnetic sensors," *Proceedings of the IEEE* , Vol. 78, No. 6, pp.973-989, 1990.

[12] D. Titterton, and J. Weston. *Strapdown Inertial Navigation Technology*. 2nd ed. Reston, VA: The American Institute of Aeronautics and Astronautics, 2004. Print.

[13] R. Figliola, and D. Beasley. *Theory and Design for Mechanical Measurements*. 4th. Hoboken, NJ: John Wiley & Sons, Inc., 2006. Print.

[14] L. Freitag, M. Johnson, M. Grund, S. Singh, J. Preisig, "Integrated Acoustic Communication and Navigation for Multiple UUVs", *Oceans Conference Record (IEEE)*, Vol. 4, pp. 2065-2070, 2001.

[15] L. Freitag, M. Grund, S. Singh, J. Partan, P. Koski, K. Ball, "The WHOI micro-modem: an acoustic communications and navigation system for

multiple platforms", *Proceedings of MTS/IEEE Oceans 2005*, Vol. 2, pp.1086 – 1092, 2995.
[16] P. Ripka, "Magnetic Sensors and Magnetometers", Artech House, 2001.
[17] P.M. Newman, "*MOOS – A Mission Oriented Operating Suite*," Department of Ocean Engineering, Massachusetts Institute of Technology, Tech. Rep., 0E2003-07, 2003.
[18] Simon, D., *Optimal State Estimation: Kalman, H∞, and Non-Linear Approaches*, Hoboken, N.J. : Wiley-Interscience, c2006.
[19] Cook, M. V.. *Flight Dynamics Principles*. New York: Wiley, 1997. Print.
[20] L.B. Jackson, "*Digital Filters and Signal Processing*", 3rd Edition, Kluwer Academic Publishers, 1996.